HYDRODYNAMIC LUBRICATION EVALUATION OF SECTOR THRUST BEARINGS

Leonardo Carpinetti Vieira, l044614@dac.unicamp.br
Katia Lucchesi Cavalca, katia@fem.unicamp.br
Laboratory of Rotating Machinery – Faculty of Mechanical Engineering – Postal Box 6122
University of Campinas - UNICAMP
13083-970, Campinas, SP, Brazil

Abstract. *The pressure generation within the lubricant fluid present in the clearance between a thrust bearing and the collar attached to the shaft has a fundamental importance to avoid contact between solid parts with axial relative motion. Any existing contact can lead to friction, wear and, as a consequence, failure of elements on a rotating machine. Therefore, in order to design an effective bearing, it is important to know how the pressure is generated in the oil film and the load capacity transmitted from the collar to the bearing throughout the fluid. Thus, it is necessary to solve the Reynolds' Equation to obtain the pressure distribution on the sections under Hydrodynamic Lubrication. Then several operation parameters can be obtained, such as, the total load capacity, lubricant fluid flow, position of the maximum pressure and so on. In order to evaluate the proposed hydrodynamic lubrication problem, a numerical solution model using the Finite Difference Method in polar co-ordinates was applied. Operation characteristics of several thrust bearings with different geometries were evaluated. The analysis allowed the comparison amongst the effects caused by the set of parameters involved, such as rotating speed, oil viscosity, film thickness and sector radii, on the results of pressure distribution and the calculated load capacity, and also the evaluation of the optimum dimensions for bearings and its influence on the component efficiency.*

Keywords: Thrust Bearings, Finite Difference Method, Reynolds' Equation, Hydrodynamic Lubrication.

1. INTRODUCTION

1.1 Thrust Bearings

Bearings are, by definition, two elements with relative motion separated by a lubricant fluid which avoids contact of solid parts and, consequently, wear and failure in rotating machines. The fluid film present in the interface of moving parts must be able to provide load capacity with the least energy waste as possible and without introducing undesired instabilities.

Thrust bearings are defined by the fact that its surfaces are perpendicular to the rotating shaft. Large axial movements of the shaft are avoided due to the pressures generated within the oil present between the bearing and a moving collar, which rotates with the shaft. In order to ensure the correct functioning of the system, the clearance where the lubricant is must be extremely small, in the order of micrometers, and the bearing must have several pads separated by grooves that provide the oil.

1.2 Historical Perspective

Pinkus and Lynn (1958) solved the Reynolds' Equation for sector thrust bearings using the finite difference method. Nevertheless, due to computational limitations, they could use only a 7 x 7 mesh, which may have introduced errors in the values of the integrated pressure. Pinkus (1956) solved the Reynolds' Equation for elliptical journal bearings by using this same method. Charnes et al. (1953) obtained a solution for a sector-type bearing with exponential oil-film shape. Sternlicht and Maginniss (1957) used computers to study the operating characteristics of journal and thrust bearings. Polar co-ordinates were used in this paper, as well as in Charnes et al. (1953) and Pinkus and Lynn (1958).

In the calculations using the finite difference method in this paper, the mesh used had at least 140 x 140 points. The number of points used depended on the dimensions of the pad analyzed.

2. THEORY AND RESULTS

2.1 Description of the Problem

Figure 1 shows the geometry of the pad of a thrust bearing in both polar and cartesian co-ordinate systems. The co-ordinate r is in the radial direction with value equal to zero in the center of the bearing; the co-ordinate θ is the angular co-ordinate and increases clock-wisely. Cartesian co-ordinates are related to the polar ones as follows: $x = r\theta$ and $y = r$.
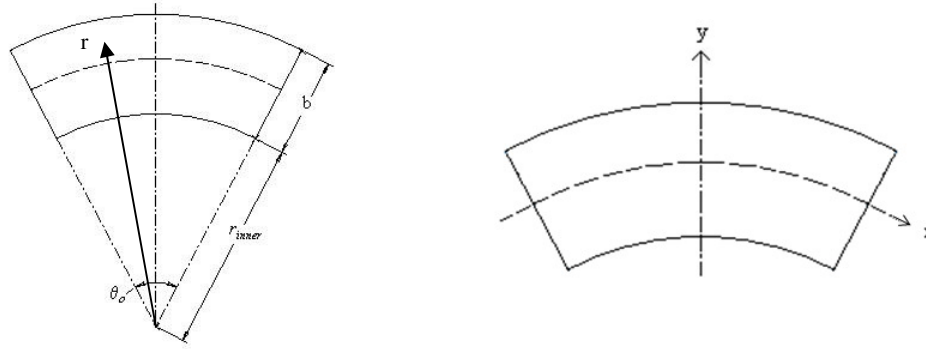
Figure 1. Polar and Cartesian Co-ordinates in a pad of a Sector Thrust Bearing

The inner radius of the pad is given by r_{inner}, the outer radius is given by r_{outer}, resulting, as a consequence, in $b = r_{outer} - r_{inner}$. The angular span of each pad is given by θ_o.

Figure 2 shows the clearance between the collar and the pad. It is important to notice that the lower surface is moving in the direction of increase of θ. This surface is the collar. The bearing will have no load capacity if the shaft rotates in the opposite direction.
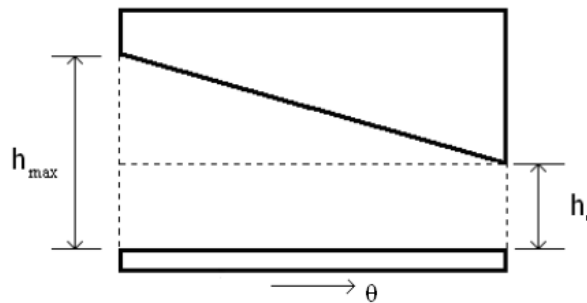
Figure 2. Shape of the oil film, governed by Equation 1

In this paper, hydrodynamic lubrication is assumed and the oil shape, as seen in Fig. 2, is given by Eq. (1), where h is the film thickness, h_o is the minimum film thickness and s_h is the difference between h_o and h_{max}, which is the maximum film thickness, as seen in Fig. 2,

$$h = h_o + s_h \left(1 - \frac{\theta}{\theta_o} \right)$$
(1)

2.2 Reynolds' Equation and Assumptions

The differential equation which governs the pressure distribution in the lubricant fluid present in the clearance between a thrust bearing and the collar attached to the shaft is called Reynolds' Equation, derived by Osborne Reynolds in his paper in 1886. It is convenient to use the Reynolds' Equation in polar co-ordinates when studying thrust bearings, as seen in Eq. (2), which is equivalent to the Reynolds' Equations used by Charnes *et al.* (1953). This equation is obtained by substituting $x = r\theta$ and $y = r$ into the Reynolds' Equation written in cartesian co-ordinates.

$$\frac{\partial}{\partial r} \left(r h^3 \frac{\partial p}{\partial r} \right) + \frac{1}{r} \frac{\partial}{\partial \theta} \left(h^3 \frac{\partial p}{\partial \theta} \right) = 6 \eta v_\theta \frac{\partial h}{\partial \theta}$$
(2)

where p is the pressure generated within the fluid, r and θ are the polar co-ordinates, as shown in Fig. 1, η is the absolute viscosity of the lubricant and v_θ is the velocity of the rotor, and consequently of the collar attached to it, in the θ direction. Constant viscosity and density, velocity of fluid in the direction of the r co-ordinate equal to zero and

pressure dependent on r and θ are assumed. As commonly used in problems related do bearings, the pressure is assumed zero on the periphery of the bearing pad. Unlike the assumptions made in the analytical model (Hamrock *et al.*, 1994 and Hamrock *et al.*, 2005), side leakages of fluid are not neglected.

2.3 Finite Difference Method

The Reynolds' Equation was solved by using the finite difference method. The position of some of the points in the mesh used in the solution can be seen in Fig. 3. It is important to notice that the index i is related to the position of a point of the mesh in the radial direction, while the index j is related to the position of a point in the circumferential direction.
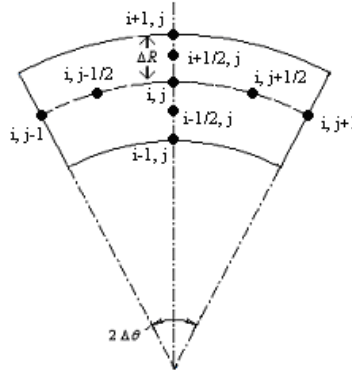
Figure 3. Mesh used in the numerical solution in Polar Co-ordinates

Incropera and DeWitt (2003) present how this method can be very useful to solve numerical problems.

Dimensionless parameters were used so that the Reynolds' Equation could be solved using less parameters and spending less computational time. The substitutions used can be seen in Eq. (3), where P, H and R are the dimensionless pressure, film thickness and radius, respectively, and N is the rotation speed of the shaft.

$$P = \frac{p(s_h)^2}{N\eta b^2} \qquad H = \frac{h}{s_h} \qquad R = \frac{r}{r_{outer}} \qquad v_\theta = 2\pi N r \qquad (3)$$

Equation (4) shows the Reynolds' Equation written in dimensionless form:

$$\frac{\partial}{\partial R}\left(RH^3\frac{\partial P}{\partial R}\right) + \frac{1}{R}\frac{\partial}{\partial \theta}\left(H^3\frac{\partial P}{\partial \theta}\right) - 12\pi R\left(\frac{r_{outer}}{b}\right)\frac{\partial H}{\partial \theta} = 0 \qquad (4)$$

Venner and Lubrecht (2000) demonstrate how the pressure gradient can be calculated for points on different positions of the mesh, especially on the periphery, where the pressure is assumed zero.

Equation (5) is obtained after writing the terms from Eq. (4) as required by the method used. Then, Eq. (5) is iteratively solved in order to obtain the values of the dimensionless pressure on each point of the mesh.

$$\frac{R_{i+1/2,j}H^3_{i+1/2,j}P_{i+1,j}}{\Delta R^2} - \frac{R_{i+1/2,j}H^3_{i+1/2,j}P_{i,j}}{\Delta R^2} - \frac{R_{i-1/2,j}H^3_{i-1/2,j}P_{i,j}}{\Delta R^2} +$$
$$+ \frac{R_{i-1/2,j}H^3_{i-1/2,j}P_{i-1,j}}{\Delta R^2} + \frac{1}{R_{i,j}}\frac{H^3_{i,j+1/2}P_{i,j+1}}{\Delta \theta^2} - \frac{1}{R_{i,j}}\frac{H^3_{i,j+1/2}P_{i,j}}{\Delta \theta^2} - \frac{1}{R_{i,j}}\frac{H^3_{i,j-1/2}P_{i,j}}{\Delta \theta^2} + \qquad (5)$$
$$+ \frac{1}{R_{i,j}}\frac{H^3_{i,j-1/2}P_{i,j-1}}{\Delta \theta^2} - 12\pi\left(\frac{r_{ext}}{b}\right)^2 R_{i,j}\left(\frac{H_{i,j+1/2} - H_{i,j-1/2}}{\Delta \theta}\right) = 0$$

2.4 Load Capacity and Optimum values

Once the dimensionless pressure has been calculated for all points in the mesh, the respective pressure can be obtained by use of Eq. (3). In addition to that, the total load capacity of one pad, which is denoted by the variable W, can be obtained by numerical integration of the pressure, using Eq. (6).

$$W = \frac{N\eta(br_{outer})^2}{(s_h)^2}\Delta\theta\Delta R\sum_i\sum_j P_{i,j}R_{i,j}$$ (6)

The optimum values of the variable θ_o are calculated by finding the best relationship between the load capacity of one pad and its area A, which can be calculated as seen in Eq. (7), with θ_o in radians.

$$A = \frac{\theta_o}{2}\left[(r_{outer})^2 - (r_{inner})^2\right] = \frac{\theta_o}{2}(r_{outer})^2\left(1-\left(1-\frac{b}{r_{outer}}\right)^2\right)$$ (7)

Pinkus and Lynn (1958) defined the dimensionless thrust factor T, which is analogous to the Sommerfeld number, used in solutions of journal bearings. This factor is essential in defining the optimum values of θ_o. Defining the term Γ, called by Pinkus and Lynn (1958) as unit loading, as seen in Eq. (8), the load capacity of the pad can then be calculated by multiplying the unit loading by the area of the pad. Finally, the thrust factor can be obtained as in Eq. (9).

$$\Gamma = \frac{W}{A} = \frac{\dfrac{N\eta b^2}{s_h^2}(r_{outer})^2\Delta\theta\Delta R\sum_1^n P_n R_n}{\dfrac{\theta_o}{2}(r_{outer})^2\left(1-\left(1-\dfrac{b}{r_{outer}}\right)^2\right)}$$ (8)

$$T = \frac{N\eta\left(\dfrac{b}{s_h}\right)^2}{\Gamma}$$ (9)

Equation (8) shows that the higher the value of Γ, the higher is the efficiency of the pad, since the rate $\dfrac{W}{A}$ is equal to Γ and, as a consequence, increases with Γ. Thus, the lower the value of T, the higher is the result of W/A, what means that for pads with different values of θ_o, the one with the best relationship between the load capacity and the area is the one with the minimum value of the thrust factor T.

Table 1. Optimum values of θ_o for different values of $\dfrac{b}{r_{outer}}$ and $\dfrac{h_{max}}{h_o}$.

h_{max}/h_o	b/r_{outer}													
	1/5	1/4	2/7	1/3	3/8	2/5	3/7	1/2	4/7	3/5	5/8	2/3	5/7	3/4
	θ_o [rad]													
2	<0,349	<0,349	0,349	0,436	0,524	0,524	0,524	0,698	0,785	0,873	0,960	1,047	1,134	1,222
3	<0,349	0,349	0,349	0,436	0,524	0,524	0,611	0,785	0,873	0,960	1,047	1,134	1,222	1,309
4	<0,349	0,349	0,436	0,524	0,524	0,611	0,611	0,785	0,960	0,960	1,047	1,222	1,309	1,396
5	<0,349	0,349	0,436	0,524	0,611	0,611	0,698	0,873	0,960	1,047	1,134	1,309	1,396	1,483
6	0,349	0,436	0,436	0,524	0,611	0,698	0,698	0,873	1,047	1,134	1,222	1,396	1,483	>1,483
7	0,349	0,436	0,524	0,611	0,698	0,698	0,785	0,960	1,134	1,222	1,309	1,483	>1,483	>1,483
8	0,349	0,436	0,698	0,611	0,698	0,785	0,785	1,047	1,222	1,222	1,396	>1,483	>1,483	>1,483
9	0,349	0,436	0,524	0,611	0,785	0,785	0,873	1,047	1,222	1,309	1,483	>1,483	>1,483	>1,483

The dimensionless rates $\dfrac{b}{r_{outer}}$, which relates the size of one pad in the radial direction and its outer radius, and $\dfrac{h_{max}}{h_o}$, which relates the maximum and the minimum film thickness, were used as parameters in order to analyze

different geometries of pads and different clearances between the bearing and the collar. Table 1 shows the results of optimum values of θ_o (the value of θ_o that results in the minimum T) obtained for several different rates $\dfrac{b}{r_{outer}}$ and $\dfrac{h_{max}}{h_o}$. It was noticed that for higher rates $\dfrac{b}{r_{outer}}$ and $\dfrac{h_{max}}{h_o}$ the minimum thrust factor is obtained for longer pads in the angular direction, what means that the optimum θ_o increases.

2.5 Lubricant Flows and Comparison with the Analytical Results

Three different lubricant flows exist in pads of operating thrust bearings: the flow of fluid into the clearance between the pad and the collar (at the beginning of the pad), the flow out of the bearing (at the end of the pad), and the side leakage of oil, which makes the fluid go out of the bearing at both inner and outer radii. Equation (10) defines the dimensionless fluid flow, Q, at any part of the bearing, obtained from the fluid flow q.

$$Q = \frac{q}{\pi r_{outer} N b s_h} \tag{10}$$

$$Q_{side\,outer} = -\frac{1}{12\pi}\left(\frac{b}{r_{outer}}\right)\sum_j H_{i,j}{}^3 R_{i,j}\left(\frac{-4P_{i-1,j}+P_{i-2,j}}{2\Delta R}\right)\Delta\theta \tag{11}$$

$$Q_{side\,inner} = -\frac{1}{12\pi}\left(\frac{b}{r_{outer}}\right)\sum_j H_{i,j}{}^3 R_{i,j}\left(\frac{4P_{i+1,j}-P_{i+2,j}}{2\Delta R}\right)\Delta\theta \tag{12}$$

Equations (11) and (12) demonstrate how the flows in the radial direction (side leakages) can be calculated by using the finite difference method. The variable $Q_{side\,outer}$ is the flow of fluid out of the bearing on the outer radius (calculated at $R=1$) and $Q_{side\,inner}$ is the flow of fluid out of the bearing on the inner radius (calculated at $R = \dfrac{r_{inner}}{r_{outer}}$). These variables were analyzed in graphics with their absolute values, since the direction of each flow is already known. Equation (13) shows how the total side flow, Q_{side}, is calculated:

$$Q_{side} = \left|Q_{side\,outer}\right| + \left|Q_{side\,inner}\right| \tag{13}$$

In order to compare the influence of the geometry and dimensions of one pad over the results of lubricant flows, the variable λ is defined as the rate of the arc length of one pad at its average radius $\left(\dfrac{r_{outer}+r_{inner}}{2}\right)$ and its length in the radial direction (the parameter b). Using θ_o in radians, Eq. (14) shows how λ was can be calculated.

$$\lambda = \theta_o \frac{(r_{outer}+r_{inner})}{2}\frac{1}{b} = \frac{l}{b} \tag{14}$$

Figures 4 and 5 show the variation of the absolute values of Q_{side} as a function of λ. It is clear, from Eq. (14), that for bearings with the same length b, higher values of θ_o result in higher values of λ. Thus, the variation of Q_{side} as function of the angular span of one pad is similar to what can be seen in Figures 4 and 5. Figure 4 also shows that the rate $\dfrac{h_{max}}{h_o}$ does not have much influence on the side flow, even though it can be noticed that higher rates produce slight increases of the side leakage. Figure 5 shows the influence of $\dfrac{b}{r_{outer}}$ over the side leakage. Higher values of $\dfrac{b}{r_{outer}}$ result in less side leakage.
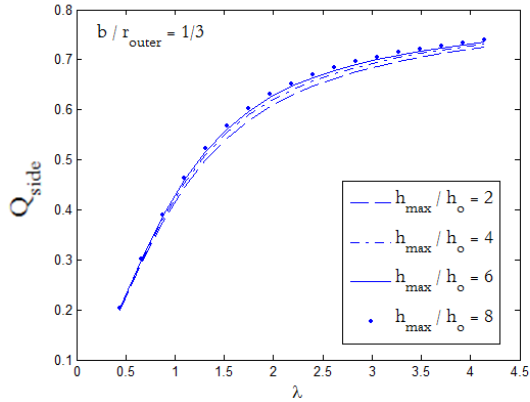
Figure 4. Q_{side} *versus* λ, plotted for $\dfrac{b}{r_{outer}} = \dfrac{1}{3}$ and different values of $\dfrac{h_{max}}{h_o}$
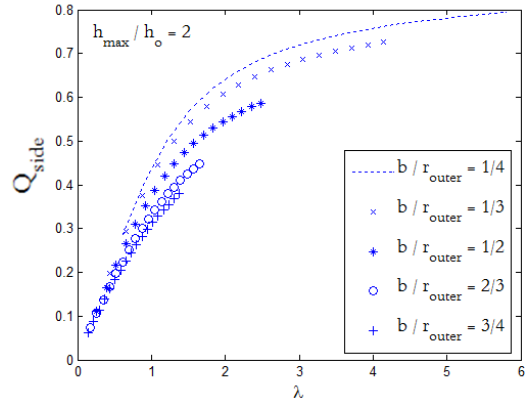
Figure 5. Q_{side} *versus* λ, plotted for $\dfrac{h_{max}}{h_o} = 2$ and different values of $\dfrac{b}{r_{outer}}$

Comparing the results of pressure distribution obtained from the numerical solution with the results obtained with the analytical model proposed by Hamrock et al. (1994), it is clear that the lower the values of λ, less side leakage occurs, what causes results of these two solutions closer to each other, as the analytical model neglects the existence of Q_{side}. The numerical results are clearly closer to what really occurs in terms of the hydrodynamic lubrication in thrust bearings than the analytical results, since the first one is calculated with much less simplifications than the second one. However, it is possible to say that the analytical model gives good qualitative results for preliminary analysis about the pressure distribution and the operational characteristics of thrust bearings.

2.6 Dimensionless Pressure Distribution and Position of the Maximum Dimensionless Pressure
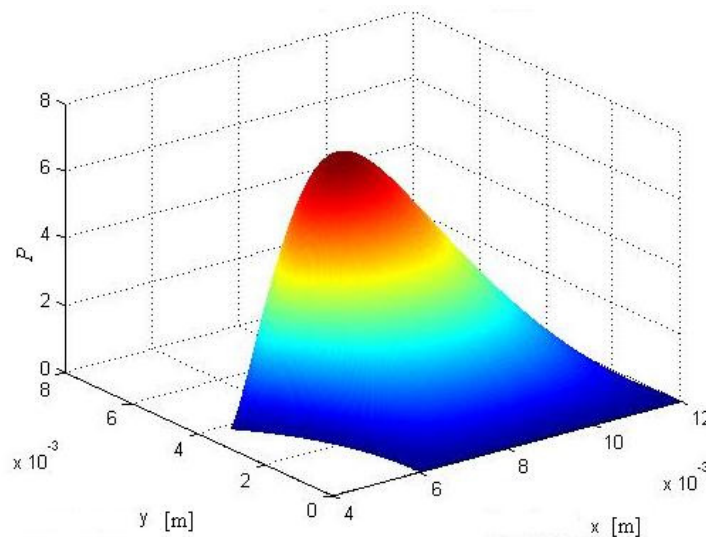
Figure 6. Dimensionless Pressure Distribution, plotted for $\dfrac{h_{max}}{h_o} = 3$ and $\dfrac{b}{r_{outer}} = \dfrac{1}{2}$

The pressure distribution along the fluid has, in general, the same shape. Although the slope or the position of the maximum pressure changes as the operational parameters, such as $\dfrac{b}{r_{outer}}$ and $\dfrac{h_{max}}{h_o}$, change, the pressure has, in

general, a similar distribution. Figure 6 shows the dimensionless pressure distribution in the fluid for one bearing operating with $\dfrac{h_{max}}{h_o} = 3$ and $\dfrac{b}{r_{outer}} = \dfrac{1}{2}$.

The position of the maximum pressure is best analyzed by introducing dimensionless variables related to its position both in the radial and the circumferential directions, called R_{max} and $\theta_{max\,adm}$, respectively. Equations (15) and (16) demonstrate how these parameters were obtained:

$$R_{max} = \frac{r_{max} - r_{inner}}{b} \tag{15}$$
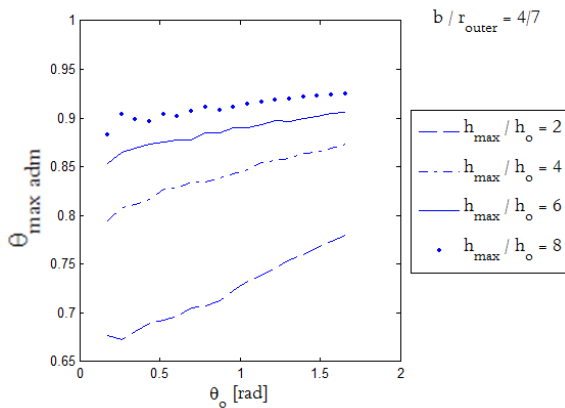
$$\theta_{max\,adm} = \frac{\theta_{max}}{\theta_o} \tag{16}$$

Figure 7. $\theta_{max\,adm}$ versus θ_o, plotted for $\dfrac{b}{r_{outer}} = \dfrac{4}{7}$ and different values of $\dfrac{h_{max}}{h_o}$

Figure 8. $\theta_{max\,adm}$ versus θ_o, plotted for $\dfrac{h_{max}}{h_o} = 2$ and different values of $\dfrac{b}{r_{outer}}$ $\dfrac{b}{r_{outer}}$
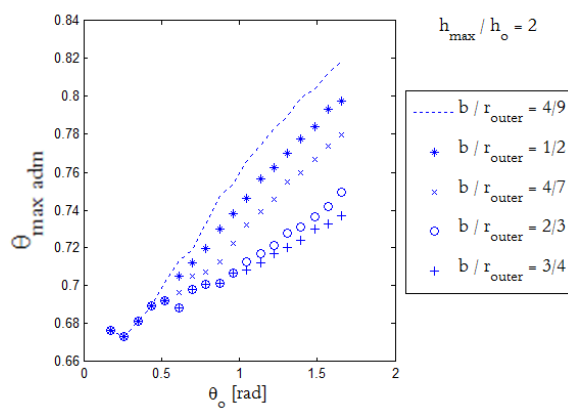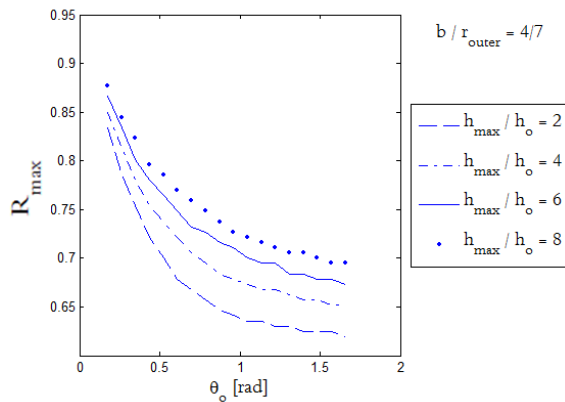
Figure 9. R_{max} versus θ_o, plotted for $\dfrac{b}{r_{outer}} = \dfrac{4}{7}$ and different values of $\dfrac{h_{max}}{h_o}$
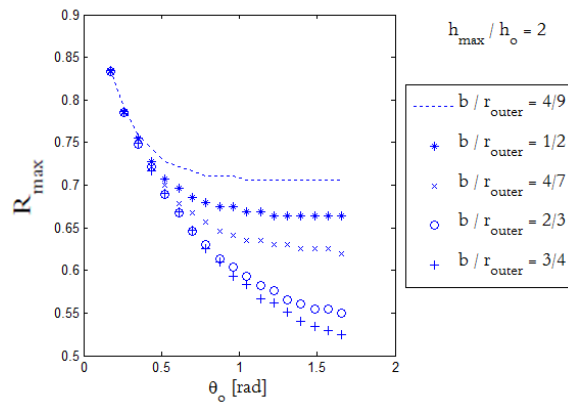
Figure 10. R_{max} versus θ_o, plotted for $\dfrac{h_{max}}{h_o} = 2$ and different values of $\dfrac{b}{r_{outer}}$

Figure 7 shows that the circumferential position of the maximum pressure, $\theta_{max\,adm}$, becomes closer to the exit of the pad as θ_o or $\dfrac{h_{max}}{h_o}$ increases. Nonetheless, the value of $\theta_{max\,adm}$ becomes smaller (the maximum pressure becomes

closer to the center of the pad) as $\dfrac{b}{r_{outer}}$ increases, what can be seen in Fig. 8. In general, the values of $\theta_{\max\,adm}$ lie between 0.6 and 0.9.

Figure 10 shows that the radial position of the maximum pressure, $R_{\max}$, becomes further from the periphery of the pad (the value of $R_{\max}$ decreases) as θ_o or $\dfrac{b}{r_{outer}}$ increases. Similarly to what happens to $\theta_{\max\,adm}$, the value of $R_{\max}$ increases as $\dfrac{h_{\max}}{h_o}$ increases, as seen in Figure 9. In general, $R_{\max}$ lies between 0.5 and 0.85.

Both Figures 8 and 10 show that the positions of the maximum pressure in the circumferential or in the radial direction depend very little on $\dfrac{b}{r_{outer}}$ when θ_o is smaller than $\theta_o = 30º$.

2.7 Maximum Dimensionless Pressure

Figure 11 shows the variation of the maximum dimensionless pressure, $P_{\max}$, as function of θ_o for different values of $\dfrac{h_{\max}}{h_o}$. Figure 12 shows the variation of $P_{\max}$ as function of θ_o for different values of $\dfrac{b}{r_{outer}}$.
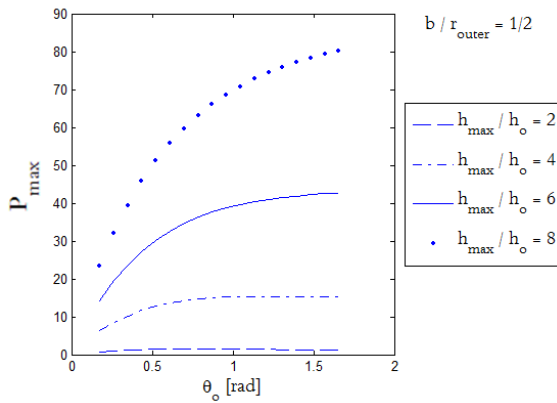
Figure 11. $P_{\max}$ *versus* θ_o, plotted for $\dfrac{b}{r_{outer}} = \dfrac{1}{2}$ and different values of $\dfrac{h_{\max}}{h_o}$
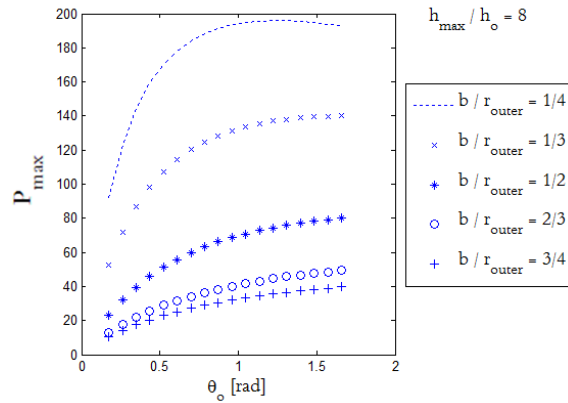
Figure 12. $P_{\max}$ *versus* θ_o, plotted for $\dfrac{h_{\max}}{h_o} = 8$ and different values of $\dfrac{b}{r_{outer}}$

It can be seen from Figures 11 and 12 that for longer pads (higher values of θ_o) the maximum dimensionless pressures have higher values. Also, as the $\dfrac{h_{\max}}{h_o}$ increases the maximum pressure also increases (Figure 11).

Figure 12 also shows that, unlike what happens when $\dfrac{h_{\max}}{h_o}$ varies, the increase in the value of $\dfrac{b}{r_{outer}}$ causes the peak pressure to diminish.

2.8 General Comments

In order to obtain other results and conclusions, some of the operational parameters, such as rotation speed, oil viscosity, film thickness, sector radii of the pad, θ_o and the rates $\dfrac{b}{r_{outer}}$ and $\dfrac{h_{\max}}{h_o}$, were varied so that the effects caused by these parameters on the fluid flows, position of the center of pressure, pressure distribution, load capacity and other characteristics of the functioning system could be analyzed.

The area of one pad is directly proportional to its load capacity in thrust bearings. This means that higher values of θ_o or higher values of b result is a higher value of W. However, a great load capacity does not mean that one specific

bearing pad has an efficient load per unit area rate. Pads with greater areas dissipate more power and have higher values of thrust factor.

Some conclusions about the effects of the variation of three parameters ($\frac{b}{r_{outer}}$, $\frac{h_{max}}{h_o}$ and θ_o) could be drawn.

Increasing the value of $\frac{h_{max}}{h_o}$ influence the characteristics of one pad with Hydrodynamic Lubrication causing the following results:
- Both the position of the center of pressure and the position of the maximum pressure on each pad become closer to the exit of the pad, in both radial and circumferential positions;
- The dimensionless pressure, P, has higher values;
- The flow of fluid into the bearing (at the beginning of the pad in the circumferential direction) and the flow out of the bearing (at the end of the pad, also in the circumferential direction) decrease; nevertheless, the side leakage increases;
- The thrust factor, T, decreases;
- The optimum θ_o becomes longer;

Increasing the value of $\frac{b}{r_{outer}} = \frac{r_{outer} - r_{inner}}{r_{outer}}$ influence the characteristics of one pad with Hydrodynamic Lubrication causing the following results:
- The position of the maximum pressure on each pad become closer to its center, in both radial and circumferential positions, which means that R_{max} and $\theta_{max\,adm}$ decrease; The position of the center of pressure in the circumferential direction also becomes closer to the center of the pad, but its position in the radial direction becomes closer to the outer radius r_{outer};
- The dimensionless pressure, P, has lower values;
- The load capacity of the bearing increases;
- All flows into and out of the bearing, in circumferential or in radial direction, decrease;
- The thrust factor, T, increases;
- The optimum θ_o becomes longer;

Increasing the value of θ_o cause the following results:
- The positions of the maximum pressure and the center of pressure in the circumferential direction becomes closer to the periphery of the pad; the positions of the maximum pressure and the center of pressure in the radial direction become closer to the center of the pad;
- The dimensionless pressure, P, has higher values;
- The load capacity of the bearing increases;
- The flow of fluid into the bearing (at the beginning of the pad in the circumferential direction) and the side leakages flow out of the bearing (at the end of the pad, also in the circumferential direction) increase; however flow out of the bearing (at the end of the pad, also in the circumferential direction) decrease;
- The values of the thrust factor, T, do not change uniformly as θ_o varies;

The influence of the fluid lubricant viscosity, η, and the rotation speed, N, were also analyzed. These parameters were found to be directly proportional to the pressure. As can be seen from Eq. (5), the dimensionless pressure distribution does not depend on the viscosity of the lubricant viscosity and the rotation speed. Therefore, the values of P do not change when the oil viscosity or the rotation are modified. Thus, dimensionless variables such as center of pressure, position of the maximum pressure and the thrust factor also remain the same. However, the dimension pressure p changes and increases if the viscosity or the rotation speed increases, as can be noticed from Eq. (3).

The maximum film thickness, h_{max}, and the minimum film thickness, h_o, also modify the characteristics of the lubrication. Increasing the value of the maximum film thickness h_{max} results in smaller load capacity and thrust factor. Increasing the value of h_o also results in a smaller load capacity but increases the thrust factor.

With regards to the positions of the maximum pressure, the center of pressure and the maximum dimensionless pressure, the influences of h_{max} and h_o are the following:

- Increasing h_{max} results in positions of the center of pressure and of the maximum pressure closer to the periphery of the pad; the maximum pressure increases;

- The minimum film thickness has the opposite influence over these parameters. In other words, increasing h_o results in positions of the center of pressure and of the maximum pressure closer to the center of the pad; the maximum pressure decreases.

3. CONCLUSIONS

The finite difference method was proposed to solve the lubrication model in sector thrust bearings in polar co-ordinates. The comparison with the analytical model shows reasonable results and the numerical model seems to present the necessary robustness to evaluate the hydrodynamic pressure distribution.

The sensitivity analysis evaluated for several design parameters of the thrust bearing makes possible the improvement of the set of parameters involved in the sector thrust bearing project, as film thickness and sector radii, concerning their effects on the maximum hydrodynamic pressure developed in the bearing pads. These effects are responsible for the supporting forces generated in the bearing gap, i.e., the thrust bearing load capacity, as well as the bearing oil leakage in the periphery boundaries.

Impact of important design parameters as radial width, tapered face angle, and angular extension of the bearing pad are discussed and the results present a good possibility of applicability as a computer aided design to this kind of rotating machinery components.

4. ACKNOWLEDGEMENTS

5. REFERENCES

Charnes, A.; Saibel E; Ying A. S. C., 1953, "On the Solution of the Reynolds´ Equation for Slider-Bearing Lubrication – V, The Sector Thrust Bearing", Transactions of the ASME, vol. 75, pp. 1125-1132.

Hamrock, B. J.; Schmid, S. R.; Jacobson, B. O., 1994, "Fundamentals of Machine Elements", McGraw Hill, 2nd ed., New York, USA, pp. 155-267.

Hamrock, B. J.; Schmid, S. R.; Jacobson, B. O., 2005, "Fundamentals of Machine Elements", McGraw Hill, 2nd ed., New York, USA, pp. 325-539.

Incropera, F. P.; DeWitt, D. P., 2003, "Fundamentals of Heat and Mass Transfer", (in Portuguese), LTC, 5th ed., pp. 130-169.

Pinkus, O., 1956, "Analysis of Elliptical Bearings", Transactions of the ASME, vol. 78, pp. 965-973.

Pinkus, O.; Lynn, W., 1958, "Solution of the Tapered-Land Sector Thrust Bearing", Transactions of the ASME, vol. 80, pp. 1510-1516.

Sternlicht B.; Maginniss F. J., 1957, "Application of Digital Computers to Bearing Design", Transactions of the ASME, vol. 79, pp. 1483-1493.

Venner, C. H.; Lubrecht, A.A.; 2000, "Multilevel Methods in Lubrication", Elsevier, Tribology Series, vol. 37, 1st ed., Netherlands, pp.1-133.

6. RESPONSIBILITY NOTICE

The authors are the only responsible for the printed material included in this paper.